Synthesis and thermal degradation kinetics of poly(propyltri(phenylethynyl)) silane

[1] De-Xin Tan, [2] Yan-Li Wang*
School of Chemistry and Chemical Engineering, Lingnan normal university.
Zhanjiang, Guangdong 524048, P R China

Abstract*— A novel propyltri(phenylethynyl)silane monomer (PTPES) was synthesized with ethyl bromide, propyltrichlorosilane and phenylacetylene by Grignard reaction. The molecular structure was characterized by FT-IR, ^{1}H-NMR, ^{13}C-NMR, and ^{29}Si-NMR. The poly(propyltri(phenylethynyl)) silane (PPTPES) was also prepared by thermal polymerization and the corresponding thermal degradation kinetics and mechanism were also studied with TG-DTG technology combining with model and model-free fitted methods. Results show that the activation energy and the pre-exponential factor were about E_a=219.69 kJ/mol and lgA=10.45 s^{-1} based on Kissinger, Ozawa, Coats-Redfern, Achar, Friedmen and Vyazovkin-Wight methods. The degradation mechanism obeyed 2D diffusion and the mechanism function were $f(\alpha)=\frac{3}{2}(1+\alpha)^{\frac{4}{3}}\left[(1-\alpha)^{-\frac{1}{3}}-1\right]^{-1}$ and $g(\alpha)=\left[(1-\alpha)^{-\frac{1}{2}}-1\right]^{2}$.

Keywords: propyltri(phenylethynyl)silane; Grignard reaction; thermal degradation kinetics; degradation mechanism

1 INTRODUCTION

Nowadays the silicon-containing arylacetylenic monomers have received much attentions because of high-performance characteristics [1]. Numerous existing literatures have reported the silicon-containing arylacetylenic monomer with different substituents at the Si bood, such as alkyl, phenyl and vinyl groups [2-4]. Wrackmeyer divides the preparation of various alkynylsilanes into two methods. One is the sophisticated reactions with the rigorous reaction conditions and the expensive raw materials (e.g. ruthenium). The other is conventional reactions of commercial chlorosilanes with alkynyllithium or ethynyl magnesium reagents [5]. Yet these main synthetic routes are dehydrogenation coupling reactions between hydrosilanes and alkynic compounds using metal compounds as catalysts, which are difficult to commercial process. However, Grignard reactions are mild and reaction conditions are easily controlled, and some silicon-containing arylacetylenic monomers were also prepared by Grignard reaction: methyltri(phenylethynyl)silane [6], vinyltri(phenylethynyl)silane, phenyltri(phenylethynyl)silane and diphenyl(diphenylethynyl)silane [7,8].

Study of thermal degradation characteristics helps us understand the thermal characteristics of materials. Currently, many researchers have studied the thermal degradation kinetics of polymers, such as polyimide, polycarbonate, bisphenol A and poly (ether ether ketone) [9-12] etc. To the best of our knowledge, very few papers have been appeared last years in the literature on the thermal degradation kinetics of arylacetylenic resins.

In this study, we synthesized propyltri(phenylethynyl)silane monomer (PTPES) using propyltrichlorosilane and phenylacetylene by Grignard reaction and made a detailed discussion about thermal degradation kinetic of poly(propyltri(phenylethynyl)) silane (PPTPES) by thermal analysis. At the same time, the thermal degradation kinetic parameters were also calculated at different heating rates of 10, 15, 25, 30 °C/min and the thermal degradation mechanism was also proposed.

2 EXPERIMENTAL

2.1 Materials

Propyltrichlorosilane and phenylacetylene was purchased from aike Reagent Company, China. Magnesium ribbons were supplied from Chengdu KeLong Chemical Reagent Company, China. Ethyl bromide and tetrahydrofuran (THF) were supplied from Tianjin Bodi Chemical Co., Ltd., China. Hydrochloric acid was bought from Reagent Chemical Industry Corporation of Shanghai, China.

2.2 Synthesis and cure of PTPES

The magnesium ribbon, THF and iodine were introduced into a three-necked 125 mL flask with condenser, dropping funnel, stirrer and nitrogen. A solution of 5 mL ethyl bromide and 20 mL THF was dropwise added about 1 h and refluxed over 3 h to produce ethylmagnesium bromide. 7.3 mL phenylacetylene and 20 mL THF were dropwise added in an ice-bath about 1 h and refluxed over 3 h to prepare the phenylethynylene Grignard reagent. Then, 3.3 mL propyltrichlorosilane and 25 mL THF were dropwise added in an ice-bath over 1 h and refluxed over 3 h. 1 mol/L solution of hydrochloric acid was gradually added and toluene and deionized water were used to wash until neutral, respectively. The solvent was distilled to get crude product and recrystallized in ethanol. PTPES was obtained (75.6% yield) (Fig. 1).

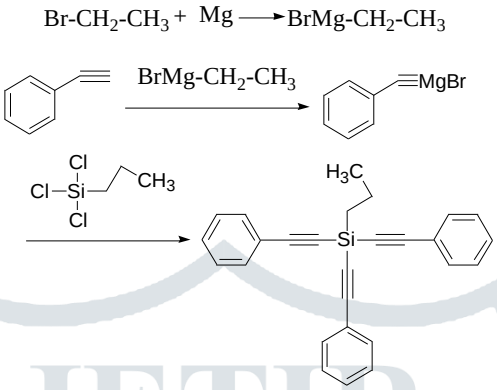

Fig. 1 Synthetic routes of the PTPES

PTPES was put into vacuum tube furnace for curing to obtained poly(propyltri(phenylethynyl)) silane (PPTPES). The curing temperature was on the basis of differential scanning calorimetry (DSC) curve at a scanning rate of 10 °C/min in nitrogen. The DSC curve was shown in Fig. 2 and the corresponding curing temperature program was following:

75 °C/1 h⟶ 290 °C /2 h⟶ 330 °C /2 h⟶ 345 °C /4 h

2.3 Characterization

A Nicolet-380 Fourier transform infrared spectrometer with a pressing potassium bromide troche method was used to measure the typical FT-IR spectra of the dried PTPES. ^{1}H-NMR, ^{13}C-NMR and ^{29}Si-NMR spectra of PTPES were traced on an AVANCE AV-400 Super-conducting Fourier Digital NMR Spectrometer (400 MHz for ^{1}H-NMR, 100.61 MHz for ^{13}C-NMR and 79.49 MHz for ^{29}Si-NMR) using tetramethylsilane as an external standard in a $CDCl_3$ solution. The TG analysis was carried out on NETZSCH TG449F3 simultaneous thermal analyzer. Samples weighing about 10.0 mg were heated from 25 to 800 °C in dynamic nitrogen environment, at different heating rates, 10, 15, 25 and 30 °C/min. The differential scanning calorimetry (DSC) study was performed on TA QA2000 in nitrogen atmosphere.

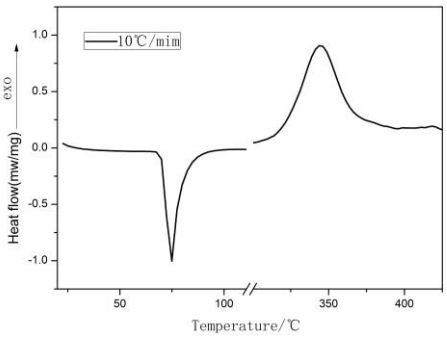

Fig. 2 A typical DSC curve of PTPES at 10°C/min heating rate

3 Results and discussion

3.1 Structural analysis of PTPES

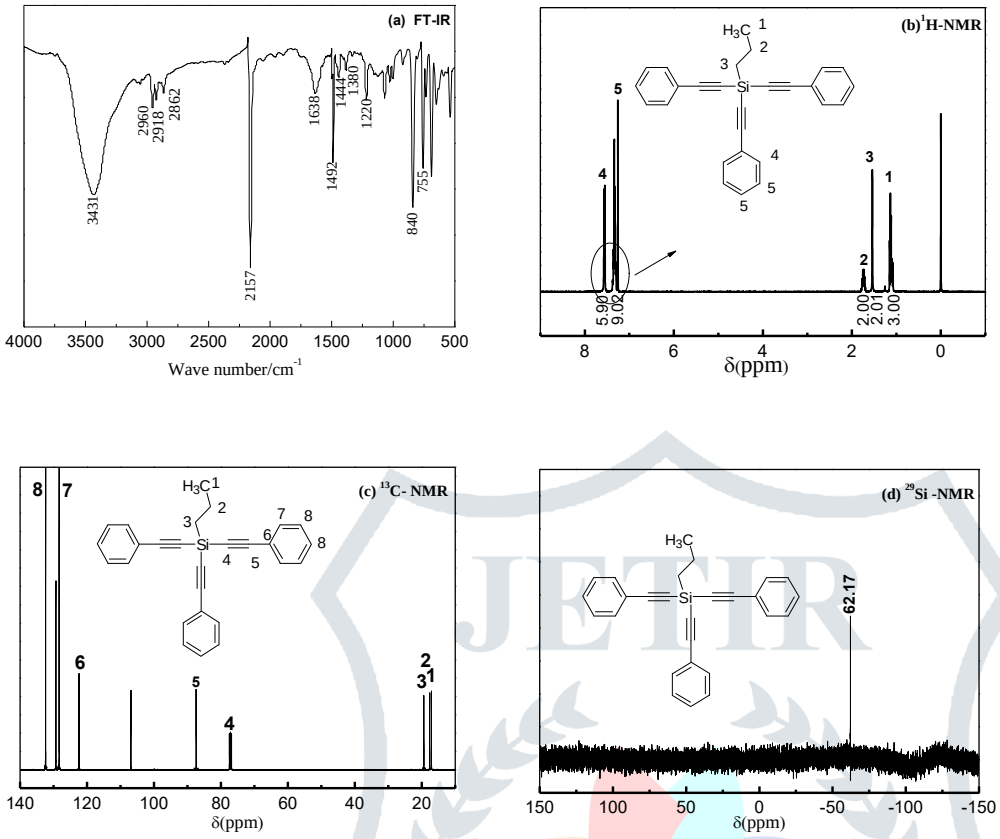

Fig. 3 Structural information of PTPES (a: FT-IR, b: ^{1}H-NMR, c: ^{13}C-NMR, d: ^{29}Si-NMR)

FT-IR spectrum of PTPES is shown in Fig. 3a. The strong peak at 2157 cm^{-1} indicates the presence of C≡C, the presence of O-H is also apparent from the absorption at 3430 cm^{-1}. The absorption bands at 2930, 2960 and 2970 cm^{-1} were assocated to C-H aliphatic stretching. Other characteristic peaks were as follows: 1491-1640 cm^{-1} (aromatic, C=C), 1067-1221 cm^{-1} (CH_2-H), 758-841 cm^{-1} (Si-C).

^{1}H-NMR spectrum of PTPES is shown in Fig. 3b. Duplet at low magnetic field (7.56 ppm) correspond to the orto-H of the ring integrating for 6 protons. The multiplet centered at 7.35 ppm is generated by meta- and para-H (total 9H). Respect to the aliphatic signals, the signal at low field (1.7 ppm, integrating for 2 H) should correspond to the CH_3CH_2-, while the multiplet at 1.05 ppm should be associated to CH_3 and Si-CH_2 protons. The nucleus directly bond to the silicon atom are displaced to high field due the low electronegativity of this heteroatom. So, Si-CH_2 protons usually appear with same displacement of a normal CH_3 group. In a precise of NMR peak integration. the ratio of ethyl protons (m, 5H, CH_3CH_2-), aromatic hydrogen (m, 6H, PhH-C≡C) adjacent to ethynyl, methylene hydrogen (m, 2H, -CH_2-) and other aromatic hydrogen (m, 9H, PhH) are in the ratio of 5:6:2:9.

The ^{13}C-NMR spectrum of the PTPES is described in Fig. 3c. The aliphatic assignations should be the following: C1 (16 ppm), C2 (19 ppm) and C3 (17 ppm) (Si-$CH_2CH_2CH_3$). The second acetylenic carbons appear as a pair of resonance at 87.40 ppm and 106.88 ppm when bonded to the silicon and phenyl unit. The aromatic carbon can be assigned: quaternary-C (121 ppm), meta-C (128 ppm), para-C (129 ppm) and orto-C (123 ppm). 29Si-NMR spectrum of PTPES is presented in Fig. 3d. The signal peaks assigned to the silicon were observed at -62.17 ppm. Based on the FT-IR, ^{1}H-NMR, ^{13}C-NMR, ^{29}Si-NMR spectra, the results were in agreement with the structure of PTPES.

3.2 Thermal stability analysis of PPTPES

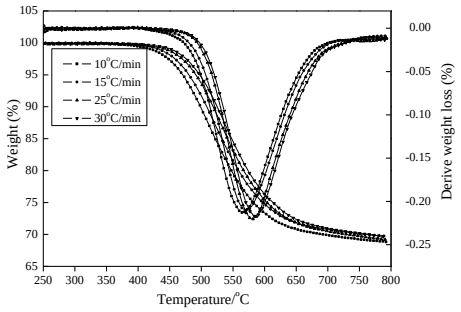

Fig. 4 TG-DTG curves of PPTPES at different heating rates

3.3 Thermal degradation kinetic analysis of PPTPES

3.3.1 Kissinger method

The thermal degradation kinetic analysis of materials is studied comprehensively from thermogravimetric results (TG) [13]. Kissinger method is a commn differential method, which uses the following Eq. (1) can roughly estimate the activation energy through the absolute temperature at the maximum thermal conversion rate of derivative thermogravimetric (DTG) curves [14]. The equation is:

$$\ln\left(\frac{\beta}{T_p^{\,2}}\right)=\ln\left(\frac{RA}{E_a}\right)-\frac{E_a}{RT_p} \qquad (1)$$

Where T_p is the peak temperature of DTG curve at different heating rate. According to the Kissinger method, the activation energies are calculated using the slope of the straight lines $\ln(\beta/T^2)$ versus 1000/T (Fig. 5). The activation energy 218.66 kJ/mol and pre-exponential factor lgA=10.47 s^{-1} are obtained.

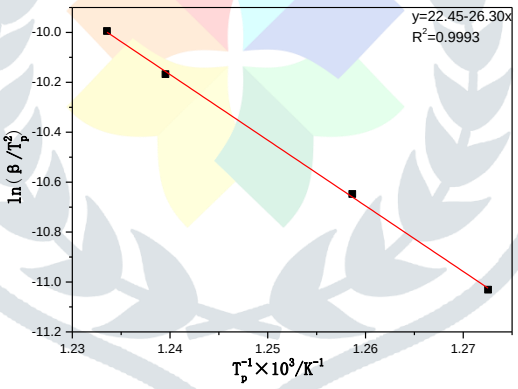

Fig. 5 $\ln(\beta/Tp^2)$ vs T_p^{-1} x10^3 of PPTPES by Kissinger

3.3.2 Ozawa method

The Ozawa method is the integral method, according to the same degree of conversion α corresponding to different temperatures at different heating rates to calculate the activation energy [15]. The equation is following Eq. (2):

$$\lg\beta=\lg\left(\frac{AE_a}{Rg(\alpha)}\right)-2.315-0.4567\,\frac{E_a}{RT} \qquad (2)$$

The characteristic parameters obtained are listed in Tab. 1 according to Fig. 6. It can be seen that correlation coefficient r^2 mostly exceeds 0.99 under the different degree of conversion α, indicating that the E_a values are reliable by Ozawa method. The average E_a value is 218.65 kJ/mol and the E_a results obtained by the Ozawa method are similar to the data from the Kissinger method (218.66 kJ/mol).

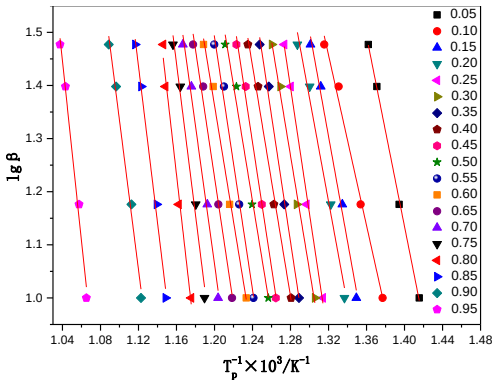

Fig. 6 lnβ vs $T_p^{-1}x10^3$ of PPTPES by Ozawa

Tab. 1 The characteristic parameters of thermal decomposition by Ozawa

α	Slope	E_a(kJ/mol)	R^2	α	Slope	E_a(kJ/mol)	R^2
0.05	-8.97	163.28	0.9993	0.55	-11.89	216.46	0.9948
0.1	-8.02	146.05	0.9943	0.6	-10.93	198.93	0.9963
0.15	-9.90	180.31	0.9955	0.65	-12.00	218.40	0.9939
0.2	-9.71	176.76	0.9906	0.7	-12.99	236.46	0.9945
0.25	-11.90	216.58	0.9974	0.75	-14.27	259.74	0.9922
0.3	-10.82	196.92	0.9959	0.8	-15.73	286.39	0.9922
0.35	-11.87	216.01	0.9964	0.85	-14.72	267.93	0.9949
0.4	-10.84	197.39	0.9943	0.9	-14.06	255.90	0.9943
0.45	-11.77	214.29	0.9963	0.95	-16.93	308.13	0.9931
0.5	-10.90	198.44	0.9923	Average		218.65	

3.3 Evaluation of degradation mechanism

3.3.1 Model fitted methods analysis

Model fitted methods can determine the thermal degradation kinetic mechanism and function combined with 30 types of thermal degradation mechanism functions (Tab.2) [16]. The thermal degradation data from the TG curves at 10 °C/min heating rate is calculated by the Coast-Redfern [17] and Achar [18] model fitted methods (Tab. 3). Preserving the activation energy Ea to satisfy $0<E_a<400$ kJ/mol [19], the probable kinetics model functions No. 9, 19, 20 are suitable. At the same time, the correlation coefficient r^2 are close to 1 and E_a and pre-exponential factor A obtained were also approached with Kissinger and Ozawa methods.

Tab. 2 Thirty types of thermal degradation mechanism functions

Mechanism	f(a)	G(a)
1	$1/2a^{-1}$	a^2
2	$-[\ln(1-a)]^{-1}$	$a+(1-a)\ln(1-a)$
3	$3/2[(1-a)^{-1/3}-1]^{-1}$	$(1-2a/3)-(1-a)^{2/3}$

4,5	$3/n(1-a)^{2/3}[1-(1-a)^{1/3}]^{-(n-1)}$	$[1-(1-a)^{1/3}]$
	n=2,1/2	n=2,1/2
6	$4(1-a)^{1/2}[1-(1-a)^{1/2}]^{1/2}$	$[1-(1-a)^{1/2}]^{1/2}$
7	$3/2(1+a)^{2/3}[(1+a)^{1/3}-1]^{-1}$	$[(1+a)^{1/3}-1]^2$
8	$3/2(1-a)^{4/3}[(1-a)^{-1/3}-1]^{-1}$	$[1/(1+a)^{1/3}-1]^2$
9	1-a	-ln(1-a)
10-16	$1/n(1-a)[-\ln(1-a)]^{-(n-1)}$	$[-\ln(1-a)]^n$
	n=2/3, 1/2, 1/3, 4, 1/4, 2, 3	n=2/3, 1/2, 1/3, 4, 1/4, 2, 3
17-22	$1/n(1-a)^{-(n-1)}$	$1-(1-a)^n$
	n=1/2, 3, 2, 4, 1/3, 1/4	n=1/2, 3, 2, 4, 1/3, 1/4
23-27	$1/n(a)^{-(n-1)}$	a^n
	n=1, 3/2, 1/2, 1/3, 1/4	n=1, 3/2, 1/2, 1/3, 1/4
28	$(1-a)^2$	$(1-a)^{-1}$
29	$(1-a)^2$	$(1-a)^{-1}-1$
30	$2(1-a)^{3/2}$	$(1-a)^{-1/2}$

Tab. 3 Calculated parameters obtained by Coats-Redfern and Achar methods at β=10°C/min

Model	Mechanism	E_a(kJ·mol^{-1})	LgA(s^{-1})	R^2
Coast-Redfern	9	208.91	7.59	0.9839
	19	281.60	12.93	0.9716
	20	379.94	19.13	0.9723
Achar	9	207.83	11.92	0.9826
	19	269.36	16.64	0.9683
	20	367.70	22.97	0.9708

According to the literature reported [20], The calculated Ea and pre-exponential factor A compared the E_a and lgA by the Coast-Redfern and Achar methods with the E_{ao} obtained by the Ozawa method, lgA_k obtained by Kissinger method, if they meet with the condition of $|(E_{ao}-E_a)/E_{ao}|\leq 0.1$, $|(lgA-lgA_k)/lgA_k|\leq 0.3$, the probable kinetic function is the best suitable kinetic degradation function. However, No. 9 is probable the best suitable kinetic model function. The average E_a values are 219.70 kJ/mol and 220.49 kJ/mol and lgA are 8.28 and 12.60 s^{-1} and the $|(E_{ao}-E_a)/E_{ao}|$ is 0.029 and 0.033 and the $|(lgA-lgA_k)/lgA_k|$ is 0.187 and 0.238 by the Coast-Redfern and Achar methods at different heating rates (Tab.4), respectively. All the results satisfy analytic conditions above mentioned. So No. 9 mechanism function is the right thermal degradation kinetic mechanism.

Tab. 4 No.9 mechanism function calculated parameters under different heating rate

Model	β	E_a(kJ/mol)	LgA(s^{-1})	R^2	$\lvert(E_{ao}-E_a)/E_{ao}\rvert$	$\lvert(lgA-lgA_k)/lgA_k\rvert$
Coast-Redfern	10	208.91	7.59	0.9839	0.045	0.255
	15	217.89	8.17	0.9843	0.003	0.197
	25	223.58	8.54	0.9818	0.023	0.161
	30	228.42	8.81	0.9819	0.045	0.134
Average		219.70	8.28	0.9830	0.029	0.187
Achar	10	207.83	11.92	0.9826	0.049	0.171
	15	218.80	12.64	0.9825	0.001	0.241
	25	224.59	12.79	0.9767	0.027	0.257
	30	230.77	13.05	0.9765	0.055	0.282
Average		220.49	12.60	0.9796	0.033	0.238

3.3.2 Model-free fitted method analysis

In order to further verify the reliability of thermal degradation kinetic mechanism, model-free methods are adopted for kinetic analysis. Two model-free methods are as follows Eqs. (3) and (4):

Friedman method [21]:

$$\ln\left(\frac{\beta d\alpha}{dT}\right) = \ln[Af(\alpha)] - \frac{E_a}{RT} \quad (3)$$

Vyazovkin-Wight method [22]:

$$\ln\left(\frac{\beta}{T^2}\right) = \ln\left(\frac{AR}{E_a g(\alpha)}\right) - \frac{E_a}{RT} \quad (4)$$

The corresponding calculated results were shown in Tab. 6 according to Fig. 7 and 8. It can be observed that the correlation coefficient r exceeds 0.99 (α range of 0.15-0.95), meaning that the calculated E_a values are reliable by Friedman and Vyazovkin-Wight methods, the average E_a is 224.60 and 216.05 kJ/mol, respectively.

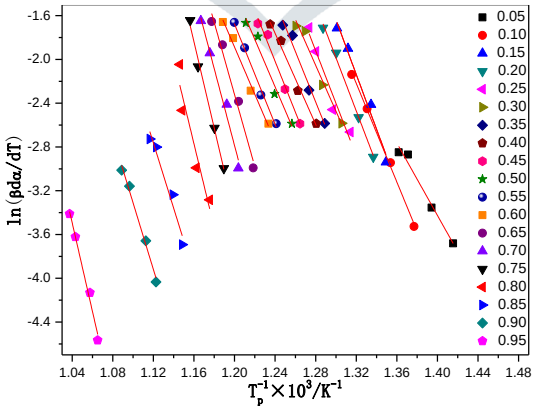

Fig. 7 ln(βdα⁄dT) vs $T_p^{-1}x10^3$ of PPTPES by Friedman

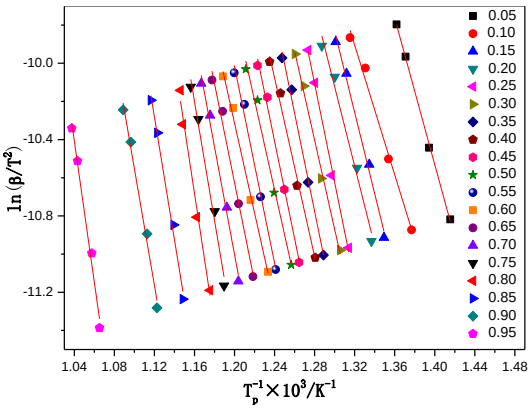

Fig. 8 $\ln(\beta/T^2)$ vs $T_p^{-1}x10^3$ of PPTPES by Vyazovkin-Wight

Tab. 6 The basic kinetic parameters acquired by Friedman and Vyazovkin-Wight

	Friedman			Vyazovkin-Wight		
α	Slope	Ea(kJ/mol)	r^2	Slope	Ea(kJ/mol)	r^2
0.05	-16.53	137.45	0.9857	-19.21	159.50	0.9992
0.10	-22.53	187.33	0.9883	-16.99	141.04	0.9932
0.15	-25.03	208.10	0.9864	-21.30	176.80	0.9948
0.20	-24.30	202.02	0.9965	-20.83	172.94	0.9902
0.25	-24.00	199.57	0.9859	-25.85	214.59	0.9971
0.30	-20.96	174.27	0.9825	-23.35	193.85	0.9953
0.35	-23.05	191.64	0.9850	-25.74	213.71	0.9959
0.40	-20.81	172.99	0.9901	-23.37	194.05	0.9935
0.45	-23.23	193.14	0.9874	-25.50	211.67	0.9958
0.50	-21.69	180.30	0.9784	-23.48	194.96	0.9912
0.55	-22.90	190.36	0.9945	-25.74	213.69	0.9941
0.60	-21.59	179.54	0.9912	-23.51	195.17	0.9958
0.65	-32.91	273.63	0.9870	-25.96	215.48	0.9925
0.70	-35.10	291.83	0.9872	-28.23	234.34	0.9938
0.75	-39.48	328.23	0.9948	-31.15	258.62	0.9913
0.80	-38.36	318.96	0.9319	-34.50	286.42	0.9914
0.85	-29.82	247.96	0.9700	-32.12	266.70	0.9943
0.90	-30.41	252.83	0.9926	-30.56	253.69	0.9936
0.95	-40.56	337.25	0.9922	-37.07	307.72	0.9923
Average		224.60			216.05	

As a result, the activation energies calculated by model-free methods (Friedman and Vyazovkin-Wight) are similar to the data

from the other four methods (Kissinger, Ozawa, Coast-Redfern and Achar method), indicating that No. 9 mechanism function is the credible thermal degradation kinetic mechanism. Namely, the mechanism is two-dimensional diffusion. The average Ea (218.66, 218.65, 219.70, 220.49, 224.60 and 216.05 kJ/mol) calculated by six methods is 219.69 kJ/mol. The average pre-exponential factor lgA (10.47, 8.28 and 12.60 s^{-1}) is 10.45 s^{-1}.

CONCLUSION

Propyltri(phenylethynyl)silane monomer (PTPES) was synthesized using the propyltrichlorosilane and phenylacetylene by Grignard reaction. The TG analysis showed that polymer PPTPES had high heat resistance property. Based on Kissinger, Ozawa, Coats-Redfern, Achar, Friedmen and Vyazovkin-Wight methods, the average activation energies E_a was 219.69 kJ/mol and average pre-exponential factor lgA is 10.45 s^{-1}. The most probable mechanism for PPTPES was 2D diffusion. The thermal degradation mechanism functions of PPTPES were $f(\alpha)=\frac{3}{2}(1+\alpha)^{\frac{4}{3}}\left[(1-\alpha)^{-\frac{1}{3}}-1\right]^{-1}$ and $g(\alpha)=\left[(1-\alpha)^{-\frac{1}{2}}-1\right]^{2}$.

Acknowledgments

This work was financially supported by the Science and Technology Innovation Special Foundation of Guangdong (No.2018A01005), the Nature Science Foundation of Guangdong (No.2017A030307028), the Yangfan Plan of Guangdong Province of China (No.0003017011) and the Research Initiation Foundation of the Lingnan Normal University (No. ZL1604, ZL1822).

References

[1] M. Cai, Q. Yuan, and F. Huang, "Catalytic effect of poly(silicon-containing arylacetylene) with terminal acetylene on the curing reaction and properties of a bisphenol A type cyanate ester," Polym. Int., Vol. 67, No.11, PP. 1563-1571, November 2018.

[2] M. Itoh, K. Inoue, K. Iwata, J. Ishikawa, and Y. Takenaka, "A heat-resistant silicon-based polymer," Adv. Mater., Vol.9, No.15, PP.1187-1190, 1997.

[3] M Chen, C Liu, and J Lin, "Correlation of cross-linked structures and properties in the characterization of dimethyl-diphenylethynyl-silane using DSC, TGA and Py-GC/MS analysis," Polym. Degrad. Stab., Vol.112, PP.35-42, February 2015.

[4] M Han, K Guo, F Wang, Y. Zhu, and H. Qi, "Synthesis, characterization, and properties of thermosets based on the cocuring of an acetylene-terminated liquid-crystal and silicon-containing arylacetylene oligomer," J. Appl. Polym. SCI., Vol.134, No.33, PP. 45141, September 2017.

[5] B. Wrackmeyer, O. L. Tok, E. V. Klimkina, and W. Milius, "Fused Silacarbacycles Containing a Silole Unit: 1,2-Hydroboration and 1,1-Organoboration of Alkynyl(vinyl)silanes," Eur. J. Inorg. Chem., Vol. 2010, No. 15, PP. 2276-2282, May 2010.

[6] D. Tan, X. Wu, Y. Wang, Y. Xu, and H. Xing, "Synthesis, characterization and curing behavior of methyl-tri(phenylethynyl)silane," Res. Chem. Intermed., Vol.42, No.5, PP.4669-4681, May 2016.

[7] D. Tan, T. Shi, and Z. Li, "Synthesis, characterization, and non-isothermal curing kinetics of two silicon-containing arylacetylenic monomers," Res. Chem. Intermed., Vol.37, No.8, PP. 831-845, October 2011.

[8] D. Tan, Y. Wang, Z. Li, and H. Xing, "Synthesis and cure kinetics of diphenyl(diphenylethynyl)silane monomer," Res. Chem. Intermed., Vol.39, No.7, PP.3427-3440, September 2013.

[9] P. E. Sanchez, L. A. Pérez, A. Perejón, and J. M. Criado, "Combined kinetic analysis of thermal degradation of polymeric materials under any thermal pathway," Polym. Degrad. Stab., Vol.94, No. 11, PP.2079-2085, November 2009.

[10] A. TCHERBI-NARTEH, M. HOSUR, E. TRIGGS, AND S. JEELANI, "THERMAL STABILITY AND DEGRADATION OF DIGLYCIDYL ETHER OF BISPHENOL A EPOXY MODIFIED WITH DIFFERENT NANOCLAYS EXPOSED TO UV RADIATION," POLYM. DEGRAD. STAB., VOL.98, NO. 3, PP.759-770, MARCH 2013.

[11] J. LI, AND S. I. STOLIAROV, "MEASUREMENT OF KINETICS AND THERMODYNAMICS OF THE THERMAL DEGRADATION FOR CHARRING POLYMERS," POLYM. DEGRAD. STAB., VOL.106, PP. 2-15, AUGUST 2014.

[12] M. N. SIDDIQUI, E. V. ANTONAKOU, H. H. REDHWI, AND D. S. ACHILIAS, "KINETIC ANALYSIS OF THERMAL AND CATALYTIC DEGRADATION OF POLYMERS FOUND IN WASTE ELECTRIC AND ELECTRONIC EQUIPMENT,"THERMOCHIM.ACTA, DOI:HTTPS://DOI.ORG/10.1016/J.TCA.2019.03.001, MARCH 2019.

[13] M. HUANG, S. LV, C. ZHOU, AND C. ZHOU, "THERMAL DECOMPOSITION KINETICS OF GLYCINE IN NITROGEN ATMOSPHERE," THERMOCHIMICA ACTA, VOL.552, PP. 60-64, JANURARY 2013.

[14] R. L. BLAINE, AND H. E. KISSINGER, "HOMER KISSINGER AND THE KISSINGER EQUATION," THERMOCHIMI. ACTA, VOL. 540, PP.1-6, JULY 2012.

[15] L. RAJABI, H. MOTAIE, A. A. DERAKHSHAN, A. R. KURDIAN, AND R. YAZDANPANAH, "DYNAMIC CURE KINETICS OF EPOXY/TIO2/MWCNT HYBRID NANOCOMPOSITES," IRAN. POLYM. J., VOL. 23, NO.11, PP.855-867, NOVEMBER 2014.

[16] Y. REN, B. CHENG, J. ZHANG, A. JIANG, AND W. FU, "THERMAL DEGRADATION KINETICS OF N, N'-DI(DIETHOXYTHIOPHOSPHORYL)-1,4-PHENYLENEDIAMINE," CHEM. RES. CHINESE UNIVERSITIES, VOL. 24, NO.5, PP. 628-631, SEPTEMBER 2008.

[17] X. LIU, Y. F. WANG, L. YU, Z. TONG, L. CHEN, H. LIU, AND X. LI, "THERMAL DEGRADATION AND STABILITY OF STARCH UNDER DIFFERENT PROCESSING CONDITIONS," STARCH-STÄRKE, VOL.65, NO.1-2, PP.48-60, JANUARY 2013.

[18] J. Z. LIANG, J. Z. WANG, GARY C. P. TSUI, AND C. Y. TANG, "THERMAL DECOMPOSITION KINETICS OF POLYPROPYLENE COMPOSITES FILLED WITH GRAPHENE NANOPLATELETS," POLYM. TEST., VOL.48, PP. 97-103, DECEMBER 2015.

[19] M. X. HUANG, C. R. ZHOU, AND X. W. HAN, "INVESTIGATION OF THERMAL DECOMPOSITION KINETICS OF TAURINE," J. THERM. ANAL. CALORIM.,VOL.113, NO.2, PP.589-593, AUGUST 2013.

[20] M. HUANG, S. LV, AND C. ZHOU, "THERMAL DECOMPOSITION KINETICS OF GLYCINE IN NITROGEN ATMOSPHERE," THERMOCHIMI. ACTA, VOL.552, PP.60-64, JANUARY 2013.

[21] H. W. Cui, J. T. Jiu, T. Sugahara, S. Nagao, K. Suganuma, H. Uchida, and K. A. Schroder, "Using the Friedman method to study the thermal degradation kinetics of photonically cured electrically conductive adhesives," J. Therm. Anal. Calorim., Vol.119, No.1, PP. 425-433, January 2015.

[22] F. Askari, M. Barikani, M. Barmar, F. Shokrolahi, M.Vafayan, "Study of thermal stability and degradation kinetics of polyurethane–ureas by thermogravimetry,"Iran. Polym. J., Vol. 24, No.9, PP. 783-789, September 2015.